Cancer Research

Bap1 Is a Bona Fide Tumor Suppressor: Genetic Evidence from Mouse Models Carrying Heterozygous Germline *Bap1* Mutations

Yuwaraj Kadariya[1], Mitchell Cheung[1], Jinfei Xu[1], Jianming Pei[1], Eleonora Sementino[1], Craig W. Menges[1], Kathy Q. Cai[2], Frank J. Rauscher[3], Andres J. Klein-Szanto[1,2], and Joseph R. Testa[1]

Abstract

Individuals harboring inherited heterozygous germline mutations in BAP1 are predisposed to a range of benign and malignant tumor types, including malignant mesothelioma, melanoma, and kidney carcinoma. However, evidence to support a tumor-suppressive role for BAP1 in cancer remains contradictory. To test experimentally whether BAP1 behaves as a tumor suppressor, we monitored spontaneous tumor development in three different mouse models with germline heterozygous mutations in *Bap1*, including two models in which the knock-in mutations are identical to those reported in human BAP1 cancer syndrome families. We observed spontaneous malignant tumors in 54 of 93 *Bap1*-mutant mice (58%) versus 4 of 43 (9%) wild-type littermates. All three *Bap1*-mutant models exhibited a high incidence and similar spectrum of neoplasms, including ovarian sex cord stromal tumors, lung and mammary carcinomas, and spindle cell tumors. Notably, we also observed malignant mesotheliomas in two *Bap1*-mutant mice, but not in any wild-type animals. We further confirmed that the remaining wild-type *Bap1* allele was lost in both spontaneous ovarian tumors and mesotheliomas, resulting in the loss of Bap1 expression. Additional studies revealed that asbestos exposure induced a highly significant increase in the incidence of aggressive mesotheliomas in the two mouse models carrying clinically relevant *Bap1* mutations compared with asbestos-exposed wild-type littermates. Collectively, these findings provide genetic evidence that *Bap1* is a bona fide tumor suppressor gene and offer key insights into the contribution of carcinogen exposure to enhanced cancer susceptibility. *Cancer Res; 76(9); 2836–44. ©2016 AACR.*

Introduction

The BAP1 cancer syndrome (Mendelian Inheritance in Man Tumor Predisposition Syndrome #614327) is caused by heterozygous germline mutation in the BRCA1 associated protein-1 gene (*BAP1*) located at chromosome 3p21.1 (1, 2). This tumor susceptibility disorder is inherited in an autosomal-dominant manner, with *BAP1* mutation carriers being at high risk for the development of a spectrum of tumor types, including atypical benign melanocytic lesions, malignant mesothelioma, uveal melanoma, cutaneous melanoma, basal cell carcinoma, meningioma, paraganglioma and carcinomas of the kidney, lung, breast, and potentially other organs (3–13). Genomic analysis of tumors from *BAP1* mutation carriers often show loss of the remaining wild-type (WT) *BAP1* allele as the second hit (4–6, 9), strongly suggesting that *BAP1* acts as a classical 2-hit tumor suppressor gene (14). The latter idea has been further supported by *in vivo* evidence using a conditional whole-body knockout mouse model, which demonstrated that somatic biallelic (homozygous) deletion of *Bap1* in adult mice recapitulates features of human myelodysplastic syndrome (15). Furthermore, mice with germline heterozygous knockout of *Bap1* ($Bap1^{+/-}$) are at increased risk of developing malignant mesothelioma when exposed to asbestos (16, 17), the main environmental factor associated with risk of this highly aggressive, treatment-resistant form of cancer. Although malignant mesothelioma is generally associated with occupational exposure to asbestos, this does not appear to be the case in malignant mesothelioma patients carrying *BAP1* mutations (4, 8, 17). Normal mesothelial cells and malignant mesothelioma cells obtained from $Bap1^{+/-}$ mice show down regulation of Rb through a p16(Ink4a)-independent mechanism, suggesting that predisposition of $Bap1^{+/-}$ mice to malignant mesothelioma is facilitated, in part, by cooperation between loss of Bap1 and Rb function (16). $Bap1^{+/-}$ mice exposed to asbestos have also been reported to have inherent alterations of the peritoneal inflammatory response, as well as a significantly higher incidence of malignant mesothelioma after exposure to low doses of asbestos that rarely induced the disease in the WT control mice (17).

While inherited inactivating mutations of *BAP1* predispose to a wide spectrum of tumors in humans and is frequently mutated in

[1]Cancer Biology Program, Fox Chase Cancer Center, Philadelphia, Pennsylvania. [2]Histopathology Facility, Fox Chase Cancer Center, Philadelphia, Pennsylvania. [3]Gene Expression and Regulation Program, Wistar Institute, Philadelphia, Pennsylvania.

Note: Supplementary data for this article are available at Cancer Research Online (http://cancerres.aacrjournals.org/).

Y. Kadariya and M. Cheung contributed equally to this article.

Current address for J. Xu: Merck Sharp & Dhome, COMSORT, 351 N Sumneytown Pike, North Wales, PA 19454.

Corresponding Author: Joseph R. Testa, Cancer Biology Program, Fox Chase Cancer Center, 333 Cottman Avenue, Philadelphia, PA 19111. Phone: 215-728-2610; Fax: 215-214-1623; E-mail: joseph.testa@fccc.edu

doi: 10.1158/0008-5472.CAN-15-3371

sporadic malignant mesothelioma, uveal melanoma, and other cancers (1, 2), the function of BAP1 in cancer is controversial (18). For example, Bott and colleagues reported that malignant mesothelioma cell lines containing wild-type BAP1 showed decreased proliferation upon *BAP1* knockdown, and that the reintroduction of wild-type *BAP1* in *BAP1*-null malignant mesothelioma cell lines resulted in an increase in cell proliferation, perplexing findings for a putative tumor suppressor gene (19). Similarly, Qin and colleagues showed that knockdown of *BAP1* in several breast cancer cell lines inhibited cell proliferation, tumorigenicity and metastasis (18).

To address experimentally whether BAP1 behaves as a tumor suppressor, we used an unbiased, genetic approach to determine whether heterozygous germline mutation of *Bap1* in mice predisposes to tumor formation. We monitored spontaneous tumor development for up to 31 months in three heterozygous mouse models with different inactivating mutations in *Bap1*. The *Bap1*-mutant mouse models included one with knockout of *Bap1* exons 6 and 7 (16), and two others with point mutations identical to those found in two human BAP1 cancer syndrome families (W and L; ref. 4), that is, a *Bap1* intron 6 splice site mutation leading to a frameshift and predicted premature stop codon and an exon 16 nonsense mutation, respectively. We report that aged mice with a germline inactivating mutation of *Bap1* are susceptible to a spectrum of spontaneous tumors, which generally differ from that observed in the human BAP1 cancer syndrome, although two *Bap1*-mutant mice did develop malignant mesothelioma. Upon exposure to asbestos, however, a very high penetrance of malignant mesothelioma was observed in the two *Bap1* knock-in models with clinically relevant germline mutations, supportive of a gene–environment interaction.

Materials and Methods

Generation of *Bap1*-mutant mice

The *Bap1* knockout mouse model has been reported previously (16). We also generated two new mouse models with inactivating *Bap1* mutations identical to those observed in the first two reported malignant mesothelioma families with germline *BAP1* mutations, that is, families W and L (4). *Bap1 W* and *Bap1 L* knock-in mice were created in a FVB genetic background using zinc finger nuclease (ZFN) technology (20), with the assistance of the Fox Chase Cancer Center (FCCC; Philadelphia, PA) Transgenic Mouse Facility, according to a strategy described previously (16). Briefly, custom ZFNs targeting different *Bap1* genomic sites were designed and validated in mammalian cells by Sigma-Aldrich. ZFN expression plasmids were linearized at the *Xba*I site located at the 3′ end of the *Fok*I ORF. The ZFN mRNAs and donor DNAs were microinjected into FVB blastocysts, which were implanted into the pseudopregnant female mice. Tails from resulting pups were genotyped by PCR amplification and sequencing to verify correct targeting. Schematic diagrams showing the cutting sites of the ZFNs and relevant portions of the respective *Bap1*-mutant alleles, as well as representative genotyping, depicted for the $Bap1^{+/W}$ (Fig. 1A) and $Bap1^{+/L}$-mutant models (Fig. 1B). Note that while the *Bap1* L knock-in mutation creates the identical stop codon seen in human family L, the *Bap1* W knock-in mouse generates a mRNA that differs from that observed in human family W (due to sequence divergence in exon 7 in human and mouse genomes); nevertheless, both encoded mRNAs result in loss of at least a portion of exon 7, and the net result is the same, that is, premature truncation of the predicted gene product.

Analysis of spontaneous tumors in *Bap1*-mutant mice

All mice were examined daily and sacrificed upon evidence of labored breathing, severe weight loss (>10% of body weight), abdominal bloating, lethargic behavior, hunched back and/or difficulty in walking, or when tumor burden was otherwise obvious, in accordance with a protocol approved by the FCCC Institutional Animal Care and Use Committee (IACUC). At the time of death, all organs were carefully examined histopathologically for evidence of tumor lesions or overt malignancy. Animals were sacrificed by CO_2 asphyxiation followed by cervical dislocation to ensure that animals euthanized with CO_2 would not revive, in accordance with IACUC guidelines. Furthermore, to assess tumor invasiveness and spreading, complete necropsies were performed on all experimental animals by opening the thoracic, abdominal, and pelvic cavities to collect tissues.

Analysis of asbestos-induced tumors in heterozygous *Bap1* knock-in mice

To assess the susceptibility of heterozygous ($^{+/mut}$) *Bap1 W* and *Bap1 L* mice to the carcinogenic effects of asbestos, cohorts of these animals and their WT littermates were injected intraperitoneally with crocidolite fibers (NIEHS grade) as reported previously (16). Briefly, male mice 10 weeks of age were anesthetized and injected with 800 μg of crocidolite in PBS every 21 days for a total of four injections. All mice were sacrificed upon signs of tumor burden as outlined above in accordance with the IACUC guidelines.

Histopathology, IHC, reverse transcriptase PCR, and immunoblotting

Formalin-fixed, paraffin-embedded (FFPE) samples were cut into 5-μm sections and mounted onto positively charged microscope slides. Sections were dewaxed in xylene and hydrated through a graded ethanol series. Heat-induced antigen retrieval was performed in 10 mmol/L sodium citrate (pH 6.0) in a microwave for 10 minutes, followed by blocking of endogenous peroxidase activity by immersion of slides in 3% H_2O_2 in PBS for 30 minutes. All H&E staining and IHC was performed by our Histopathology Facility, and all histopathologic assessments were independently performed by two experienced experimental animal pathologists (A.J. Klein-Szanto and K.Q. Cai). Markers used to confirm the diagnosis of malignant mesothelioma included mesothelin antibody D-16: sc-27702 and WT1 antibody C-19: sc-192, both from Santa Cruz Biotechnology, and pan-cytokeratin antibody Z0622 from Dako. Bap1 expression in the mouse was assessed using an antibody A302-242A from Bethyl Laboratories, whereas BAP1 expression in human ovarian sex cord stromal tumors (SCST) was determined using antibody C-4: sc-28383 (Santa Cruz Biotechnology). To confirm the granulosa cell origin of ovarian SCSTs, we used an α-inhibin antibody (MCA951ST) from AbD Serotec. Following incubation of slides with the designated antibodies, detection was with biotinylated secondary antibodies with immunodetection performed using the Dako Envision+ polymer system. The slides were then washed, counterstained with hematoxylin, dehydrated with alcohol, cleared in xylene, and mounted. Murine samples that were shown previously to express high levels of each protein investigated were used as positive controls. As a negative control, the primary antibody

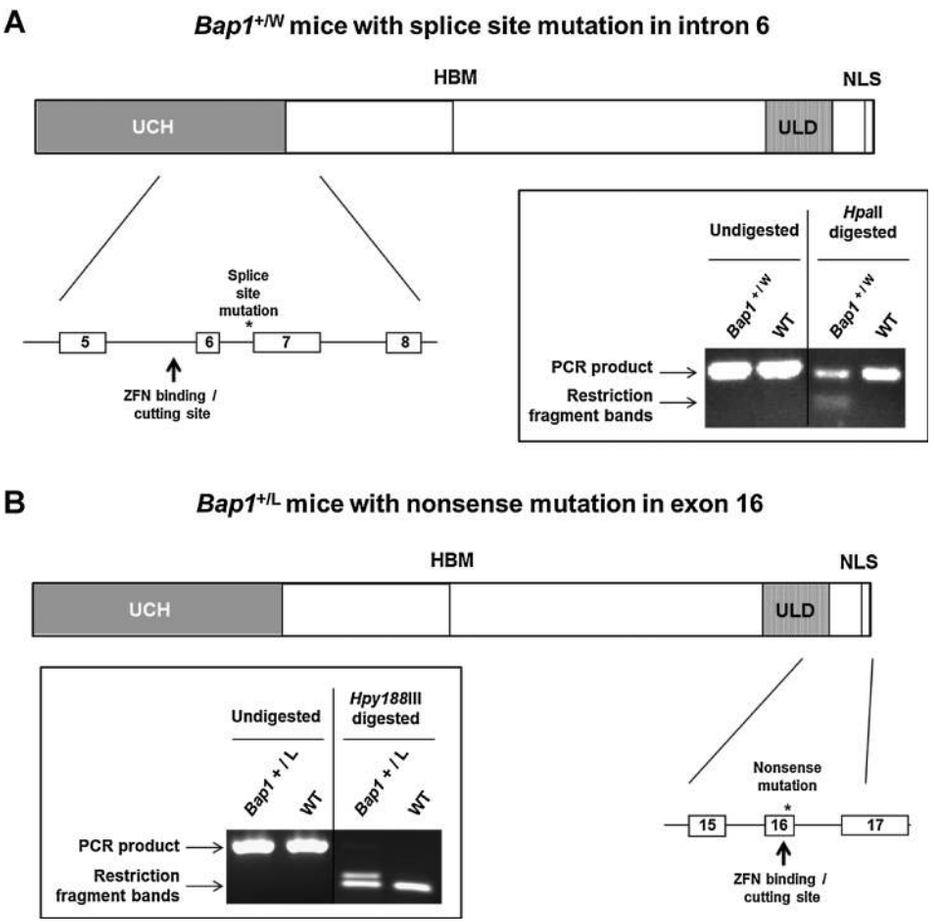

Figure 1.
Schematic diagrams showing cutting sites of the zinc-finger nucleases (ZFN) and relevant portions of the respective *Bap1*-mutant alleles, along with genotyping, for $Bap1^{+/W}$ (A) and $Bap1^{+/L}$ (B) mutant models.

was replaced with normal mouse/rabbit IgG to confirm absence of specific staining.

For some tumors, reverse transcriptase PCR (RT-PCR) analysis of markers for malignant mesothelioma, including mRNAs encoding mesothelin, E-cadherin, N-cadherin, and cytokeratin 18/19, was assessed as described previously (21). As a control, *Gapdh* was used to assess template integrity. Immunoblot analysis was used to determine expression of Bap1, using an antibody from Bethyl Laboratories. As a loading control, β-actin expression was assessed, using an antibody from Santa Cruz Biotechnology.

Laser capture microdissection and assessment of *Bap1* loss in isolated malignant mesothelioma cells

For laser capture microdissection (LCM), 5-μm sections of FFPE tumor tissue were cut and stained with H&E for histopathologic assessment and confirmation of diagnosis. Once confirmed, 10-μm sections were cut and placed on Leica Microsystems RNase-free polyethylene naphthalate (PEN)-membrane slides. The resulting FFPE sections were stained with H&E and dehydrated in 100% ethanol (Histogene LCM Staining Kit, Life Technologies). LCM was performed using a Leica Gravity, contact-free collection system (LMD 6500). Isolated tumor cells were dropped immediately into PicoPure (Life Technologies) DNA extraction buffer and incubated at 42°C for 30 minutes. Following incubation, samples were stored at −80°C until the time of DNA isolation. To assess *Bap1* allelic loss in LCM-isolated tumor cells from a spontaneous malignant mesothelioma, DNA was extracted using an AllPrep DNA/RNA FFPE Kit from Qiagen. Matching tumor and tail DNA were used as templates to amplify a portion of the mouse *Bap1* gene in the region encompassing exons 6 and 7, using PCR with primers previously described for genotyping purposes (16). The Bio-Rad Quantity One program was used to quantitate the intensity of the larger WT (634 bp) *Bap1* allele PCR product and the smaller knockout allele PCR product (158 bp). The ratio of WT to mutant band intensities was then determined for each sample.

Array-based comparative genomic hybridization analysis

To identify genomic imbalances in frozen ovarian SCSTs from *Bap1*-mutant mice, array-based comparative genomic hybridization (aCGH) analysis was performed with 244K genomic DNA arrays from Agilent, as described previously (22). Briefly, genomic DNA was isolated from matched tumor and tail tissues, restriction enzyme digested, fluorescently labeled, purified, and hybridized to Agilent arrays. After scanning of chips on an Agilent scanner, data were extracted using Feature Extraction Software, and output was imported into CGH Analytics for DNA Copy Number Analysis (Agilent).

Table 1. Spontaneous primary malignant tumor types observed in *Bap1*-mutant mice[a]

Tumor types	$Bap1^{+/-}$	$Bap1^{+/L}$	$Bap1^{+/W}$	Total tumors[b]
Ovarian SCST	8	14	16	38
Lung carcinoma	4	1	2	7
Mammary carcinoma	3	1	2	6
Spindle cell tumor	2	3	1	6
Malignant mesotheliomas	1	0	1	2
Lymphoma	0	2	0	2
Colon carcinoma	1	0	0	1
Harderian gland carcinoma	0	1	0	1
Uterine adenocarcinoma	0	1	0	1
Islet cell tumor	0	0	1	1

[a]Among 43 wild-type ($Bap1^{+/+}$) littermates (not summarized here), two had mammary carcinoma and two others had lung carcinoma.
[b]Overall number of tumors (66) is greater than the number of mice with cancer (55), because 11 *Bap1*-mutant mice had two independent primary tumors involving different organs. In addition, 12 ovarian SCSTs were bilateral.

Results

Mice with various germline-inactivating mutations of *Bap1* develop a high incidence and similar spectrum of tumor types

Creation of our *Bap1* knockout mouse model was described previously (16), and at the time of our earlier report only one spontaneous tumor, a mammary carcinoma, had been detected, although most of the mice were less than 14 months of age. For this report, we continued to age these same *Bap1* knockout mice as well as several additional litters from this model. We also generated two new knock-in mouse models with inactivating *Bap1* mutations identical to those observed in the first two reported malignant mesothelioma families with germline *BAP1* mutations, that is, families W and L (4).

Unexposed WT mice and animals with the three different germline *Bap1* mutations were followed for up to 31 months. No tumors were observed prior to 1 year of age in either WT or *Bap1*-mutant mice. Mice were sacrificed according to IACUC guidelines as outlined above, and among all mice sacrificed due to signs of illness, malignant tumors were identified in 54 of 93 (58%) *Bap1*-mutant mice compared with only 4 of 43 (9%) WT littermates (Supplementary Table S1). Most tumors in mutant mice developed late in life (median age at time of detection: 19.7 months). Eleven *Bap1*-mutant mice had two synchronous primary tumors involving different organs (54 + 11 = 65 primary tumors overall). All three *Bap1* mouse models exhibited an increased incidence and similar spectrum of tumor types, with ovarian SCSTs, lung adenocarcinomas, mammary gland carcinomas, and spindle cell tumors of the skin being seen in each of the *Bap1*-mutant models. Among the WT littermates, the 4 cancers observed included 2 lung and 2 mammary carcinomas. A summary of the types of spontaneous malignant tumor types observed to date in *Bap1*-mutant mice is presented in Table 1 and Fig. 2. In addition to malignant tumors, 7 *Bap1*-mutant mice and 9 WT mice had benign lesions, which were primarily (11/16) lipomas and adenomas of the lung.

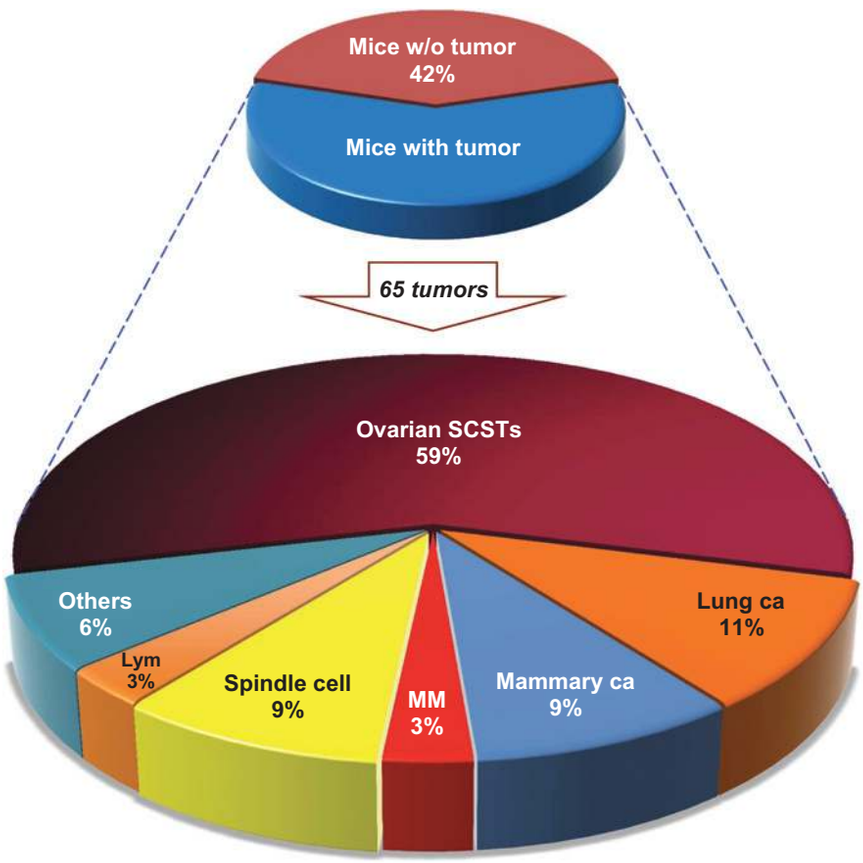

Figure 2.
Collective spectrum of spontaneous tumors observed in all three *Bap1*-mutant mouse models. Top pie chart depicts percentages of mice with or without tumors. Bottom pie chart indicates percentages of different primary tumors observed. Altogether, neoplastic tumors were identified in 54 of 93 (58%) *Bap1*-mutant mice. A total of 65 different primary tumors were found in the 54 mice, with 11 mice having two different primary tumors. Mice with bilateral ovarian SCSTs are counted here as one tumor. Percentages of different tumor types refer to proportion of all 65 tumors. MM, malignant mesothelioma; Lym, lymphoma.

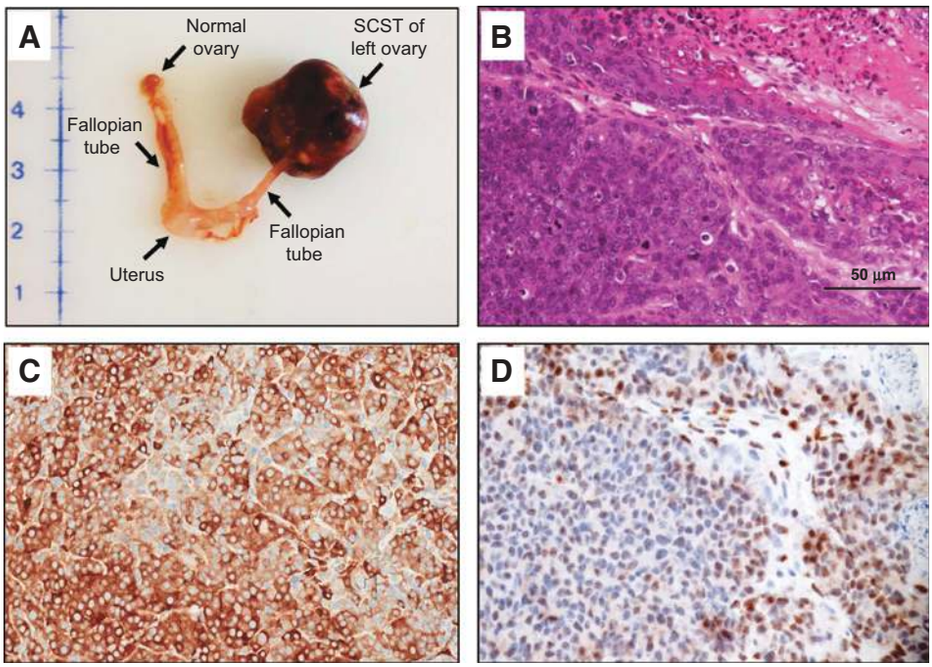

Figure 3.
Representative spontaneous ovarian SCSTs from a *Bap1*$^{+/W}$ mouse. A, macroscopic view of ovarian SCST, normal ovary, fallopian tubes, and uterus. B, H&E staining of same ovarian SCST. C, cytoplasmic α-inhibin staining indicating granulosa cell origin of same tumor. D, IHC for Bap1 showing loss of nuclear staining in most tumor cells. Panels B and D are from serial tissue sections. Original images for B–D were at ×400 magnification. Representative 50 μm scale bar is shown at bottom right in B.

The most frequent neoplasms observed in *Bap1*-mutant mice were ovarian SCSTs, which were identified in 38 of 60 (63%) females, with 8 to 16 affected animals found in each of the three *Bap1*-mutant mouse models. These neoplasms were mainly granulosa cell tumors (Fig. 3A–D) followed by mixed tumors of various cell types and occasional thecomas. Twelve females showed bilateral ovarian SCSTs. Among the 38 *Bap1*-mutant mice with ovarian SCSTs, 11 showed multiple distant metastases. Ovarian SCSTs were not observed in any of the WT females.

Two spontaneous malignant mesotheliomas were identified in *Bap1*-mutant mice, whereas none were found in any of the 43 WT mice sacrificed to date, although this difference in malignant mesothelioma incidence was not statistically significant ($P > 0.05$). Both of these spontaneous malignant mesotheliomas were sarcomatous (1 pleural; 1 peritoneal), with one found in a *Bap1*$^{+/-}$ knockout mouse and the second in a *Bap1*$^{+/W}$ knock-in mouse. The invasiveness and confirmation of the diagnosis by IHC of these two spontaneous malignant mesotheliomas are depicted in Fig. 4. Loss of Bap1 staining in one of these tumors is shown in Supplementary Fig. S1. One of the malignant mesotheliomas was diffusely spread throughout the peritoneal cavity and pelvis, with invasion of mesentery and various organs such as the pancreas (Fig. 4A–C) and seminal vesicles. The second malignant mesothelioma originated in the parietal pleura and invaded the mammary gland (Fig. 4D–F) and chest wall. An ovarian SCST was also observed in the latter mouse, but this neoplasm had a different staining pattern, that is, negative for mesothelin and WT1. Notably, the ovarian SCST contained ovoid and cuboid cells that did not stain for WT1 or mesothelin, while the sarcomatous malignant mesothelioma in the same animal exhibited spindle-shaped cells that stained positively for both of these markers (Fig. 4D–F). Thus, we concluded that this animal had two different primary tumors. Neither of the *Bap1*-mutant mice with malignant mesothelioma exhibited a pleural or peritoneal effusion.

Other recurrent cancers in *Bap1*-mutant mice included 7 lung adenocarcinomas and 6 mammary adenocarcinomas or adenosquamous cell carcinomas. In addition, 6 *Bap1*-mutant mice developed cutaneous spindle cell tumors that originated in the skin of the ear, thorax, or penis. None of the spindle cell skin tumors stained positively for S-100 or HMB-45, markers that are typically positive for melanocytes.

Spontaneous tumors in *Bap1*-mutant mice show biallelic inactivation and loss of expression of Bap1

To test whether *Bap1* haploinsufficiency is capable of fostering ovarian SCST formation or, instead, requires biallelic inactivation, aCGH analysis was performed on four ovarian SCSTs. Three of the four ovarian SCSTs tested showed loss of one copy of chromosome 14, where the mouse *Bap1* locus resides (Fig. 5A), and immunoblot analysis revealed loss of Bap1 expression in these same tumors (Fig. 5B).

The amount of tissue available for spontaneous malignant mesotheliomas was insufficient for aCGH analysis. However, in one of these malignant mesotheliomas, we were able to PCR-amplify genomic DNA from tumor cells isolated by LCM (Fig. 6A and B), which was then used for DNA sequencing of *Bap1*. PCR analysis of DNA from this spontaneous malignant mesothelioma showed markedly reduced signal for the residual WT *Bap1* allele, indicative of biallelic inactivation (Fig. 6C, left). Thus, as in our earlier studies of asbestos-induced malignant mesotheliomas in *Bap1*$^{+/-}$ mice (16), development of spontaneous malignant mesotheliomas in *Bap1*-mutant mice showed a similar mechanism of biallelic inactivation.

Mice with clinically relevant germline mutations of *Bap1* show increased susceptibility to the carcinogenic effects of asbestos

To determine whether mice with clinically relevant germline mutations of *Bap1* show increased susceptibility to asbestos,

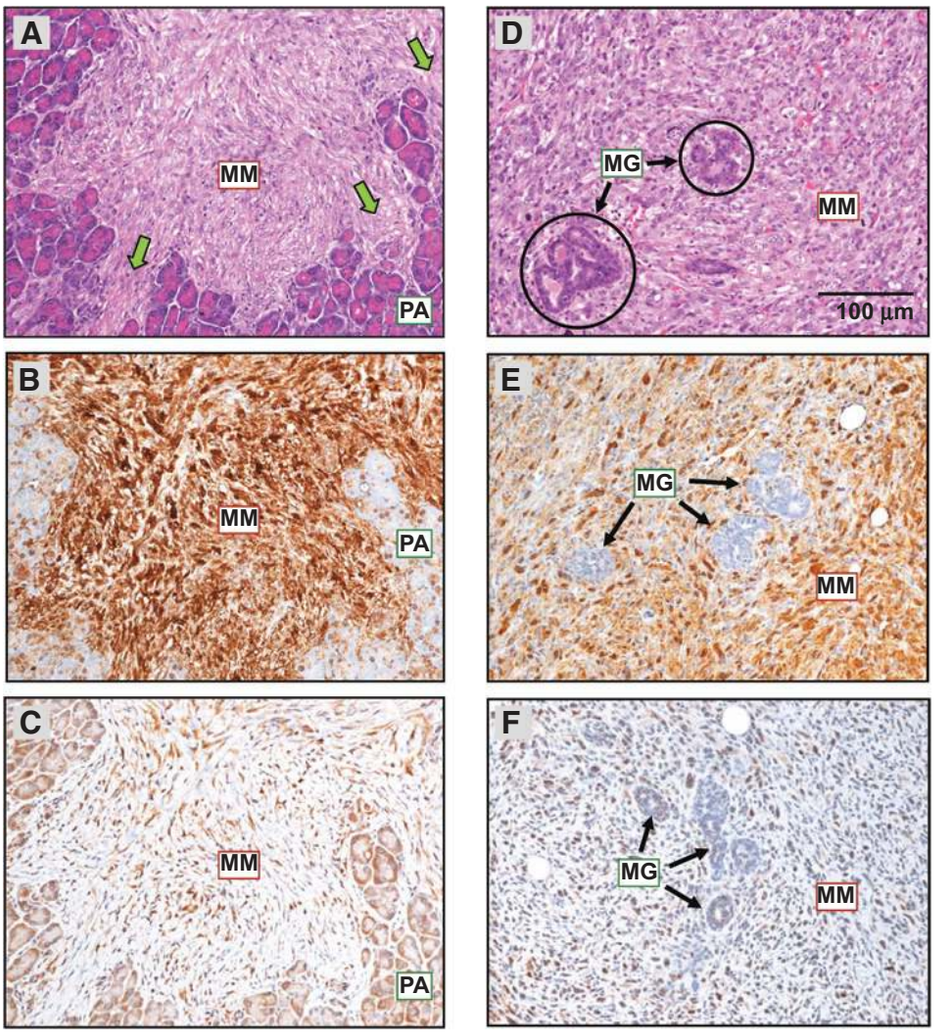

Figure 4.
Spontaneous malignant mesotheliomas (MM) seen in a $Bap1^{+/-}$ mouse (A–C) and a $Bap1^{+/W}$ mouse (D–F). A and D, H&E staining showing MM invasion into pancreas and mammary gland, respectively. Green arrows, invasion of pancreatic tissue by MM. IHC of the same tumors showing positive staining for mesothelin (B and E) and nuclear WT1 (C and F). Original images, ×200 magnification. Representative 100 μm scale bar is shown in D. Note that this is the same tumor as in Fig. 6A and B, which shows invasion of the malignant mesotheliomas into the pancreatic parenchyma at a lower magnification. MG, mammary gland; PA, pancreatic acini.

cohorts of $Bap1^{+/W}$ and $Bap1^{+/L}$ knock-in animals, and their WT littermates, were chronically injected intraperitoneally with crocidolite asbestos fibers and monitored over a period of up to 88 weeks. Approximately 70% of the *Bap1*-mutant animals eventually showed abdominal distention and most were found to have ascites when sacrificed. A few others had abdominal swelling because of intestinal distention. Almost all of these mice showed intestinal adhesions, as well as fibrous thickenings of the peritoneum, mesentery, and diaphragm undersurface, frequently with asbestos-induced plaques and granulomas involving the liver capsule and pancreas. The *Bap1*-mutant mice were found to succumb to disease much earlier than their WT littermates, with a median survival of 48 weeks in $Bap1^{+/W}$ mice and 46 weeks in $Bap1^{+/L}$ mice from the time of the first asbestos injection versus 60 weeks in WT mice (Fig. 6D), which was highly significant (Fisher exact test, $P < 0.005$ for WT vs. $Bap1^{+/W}$ mice; $P < 0.008$ for WT vs. $Bap1^{+/L}$ mice). Peritoneal malignant mesotheliomas occurred in 74% of $Bap1^{+/W}$ mice and 71% of $Bap1^{+/L}$ mice compared with 35% of WT animals. The percentage of malignant mesotheliomas in WT mice was nearly identical to that of WT control mice in a previous study using FVB mice and a comparable exposure with asbestos (16). Histopathologic assessment revealed that more than 90% of the malignant mesotheliomas in WT and *Bap1*-mutant mice were sarcomatous or biphasic in nature. Other causes of death in WT and *Bap1*-mutant mice included asbestos-related organ failure or intestinal obstructions due to mesenteric fibrosis. As previously reported for our asbestos-exposed *Bap1* knockout mice (16), asbestos-induced malignant mesotheliomas seen in both *Bap1* knock-in models were consistently larger and more aggressive than those observed in WT littermates, often with invasion to the pancreas, liver, and/or intestinal smooth muscle. In addition, we found that malignant mesotheliomas from asbestos-exposed knock-in mouse models show loss of the wild-type *Bap1* allele (Fig. 6C and Supplementary Fig. S2), indicative of biallelic inactivation.

Discussion

The BAP1 cancer syndrome is a newly recognized cancer susceptibility syndrome that is inherited in an autosomal-dominant pattern. Carriers of heterozygous *BAP1* mutations are at high risk for the development of a variety of tumors, including benign melanocytic tumors and various malignant tumors, including malignant mesothelioma, uveal, and cutaneous melanomas, as

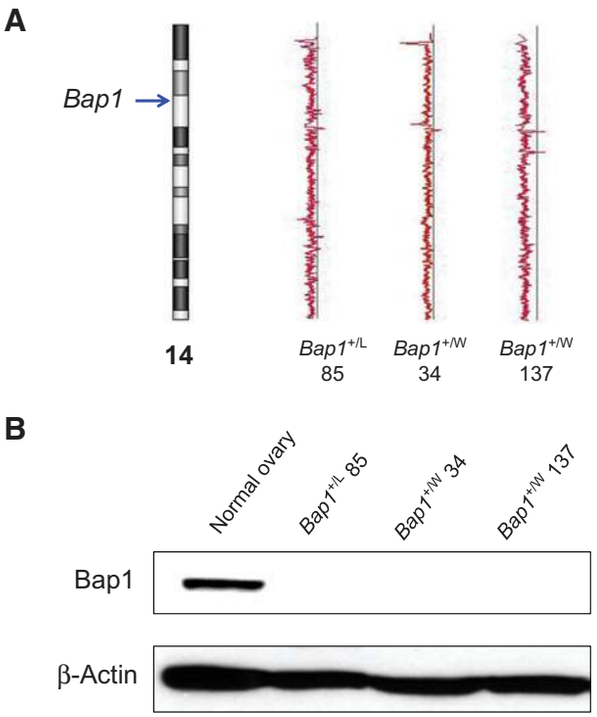

Figure 5.
Molecular analysis of Bap1 in spontaneous ovarian SCSTs from several *Bap1*-mutant mice. A, aCGH analysis depicting loss of one copy of chromosome 14, including the *Bap1* locus (arrow), in three ovarian SCSTs is shown. Note that copy number loss deviations from the "2-copy" straight line is less obvious in tumors 85 and 34 than in tumor 137, due to mosaicism or the presence of contaminating normal stroma in the former tumors. B, immunoblot analysis depicting loss of expression of Bap1 in the same ovarian SCSTs.

well as other cancer types, such as lung adenocarcinoma, meningioma, and renal cell carcinoma (2, 4–6, 9). Importantly, the *in vivo* studies presented here, using three separate mouse models, clearly demonstrate that heterozygous germline truncating mutations of *Bap1* predispose to a spectrum of malignant tumors. Moreover, the spectrum of tumors observed in the three different *Bap1*-mutant mouse models, all in the same FVB background, was similar irrespective of the type or location of the inactivating mutation. However, the generally distinct spectrum of tumors observed in our *Bap1*-mutant mice highlights differences in target tissue susceptibility between mice and humans. With the exception of two malignant mesotheliomas, other malignancies commonly observed in the BAP1 cancer syndrome, that is, uveal and cutaneous melanomas and renal cell carcinomas were not seen in mice with a germline *Bap1* mutation. Instead, a high incidence of ovarian SCSTs was observed in *Bap1*-mutant female mice. Such discrepancies between humans and mice are certainly not unprecedented. For example, Neurofibromatosis type II (NF2) is a dominantly inherited human disorder characterized by a predisposition to multiple benign tumors of the central nervous system in connection with germline mutation of the *NF2* gene, whereas mice with heterozygous knockout of *Nf2* frequently (63%) developed osteosarcoma (23), a tumor type that is not observed in NF2 disorder. Similarly, while germline mutations of *RB1* predispose to hereditary retinoblastoma in humans, $Rb^{+/-}$ mice instead exhibit a high incidence (60%–80%) of thyroid cancer and pituitary adenocarcinoma (24).

These data firmly establish in three independent experimental models that *Bap1* is a *bona fide* tumor susceptibility gene. While the spectrum of tumors observed in our mouse models generally differs from that of the human disorder, it is notable that two spontaneous malignant mesotheliomas were observed in our *Bap1*-mutant mice. Although several *Bap1*-mutant mice developed skin tumors, these were of the spindle cell type and did not appear to be of melanocytic origin. Thus, collectively, these data suggest that the finding of malignant mesotheliomas in both the human BAP1 syndrome and in *Bap1*-mutant mice is noteworthy.

While a high incidence of spontaneous ovarian SCSTs was observed in *Bap1*-mutant mice, such ovarian tumors were not found in WT littermates. In humans, ovarian SCSTs are rare ovarian tumors representing approximately 7% of all ovarian malignancies (25). To our knowledge, ovarian SCSTs have not been reported in BAP1 cancer syndrome families to date. IHC analysis of 12 deidentified human ovarian SCSTs available in the FCCC Biosample Repository revealed loss of nuclear BAP1 expression in about 50% of tumor cells from two cases, both of which were of the granulosa cell type; DNA sequencing on matched blood samples revealed no mutations of *BAP1* in either of these cases, indicating an absence of a predisposing germline *BAP1* mutation.

Although the incidence of spontaneous malignant mesothelioma was low in *Bap1*-mutant mice, a very high incidence of aggressive malignant mesotheliomas was observed following chronic exposure of these mice to asbestos. Deaths due to peritoneal malignant mesothelioma occurred in 74% of $Bap1^{+/W}$ mice and 71% of $Bap1^{+/L}$ mice, compared with 35% of WT littermates. A similar highly increased incidence of malignant mesothelioma has been observed in asbestos-exposed *Bap1* knockout mice compared with WT mice (16, 17). For example, in mice with deletion of *Bap1* exons 6 and 7, asbestos-induced malignant mesotheliomas were observed in 73% of these knockout mice versus 32% in WT littermates (16). Moreover, a significantly higher incidence of malignant mesothelioma has been reported in *Bap1*-mutant mice upon exposure to low doses of asbestos that rarely caused the disease in WT mice (17).

Unlike the malignant mesotheliomas seen in asbestos-exposed *Bap1*-mutant and WT mice, spontaneous malignant mesotheliomas observed in unexposed *Bap1*-mutant mice were not extremely invasive. Moreover, the spontaneous malignant mesotheliomas seen in *Bap1*-mutant mice were found only in relatively old animals (19 and 29 months of age) that showed severe weight loss without an accumulation of ascitic fluid. In contrast, malignant mesotheliomas observed in asbestos-exposed mice tended to be large masses that frequently involved severe infiltration of the intestinal serosa and viscera, with peritoneal effusions and occasional involvement of the chest cavity.

Collectively, our *in vivo* studies, using three different mouse models, indicate that germline inactivating mutations of *Bap1* predispose to a spectrum of malignant tumors, including occasional malignant mesotheliomas. While the incidence of frank spontaneous malignant mesotheliomas in *Bap1*-mutant animals was low (2/93; 2.2%), the penetrance of aggressive malignant mesotheliomas was very high (>70%) in *Bap1*-

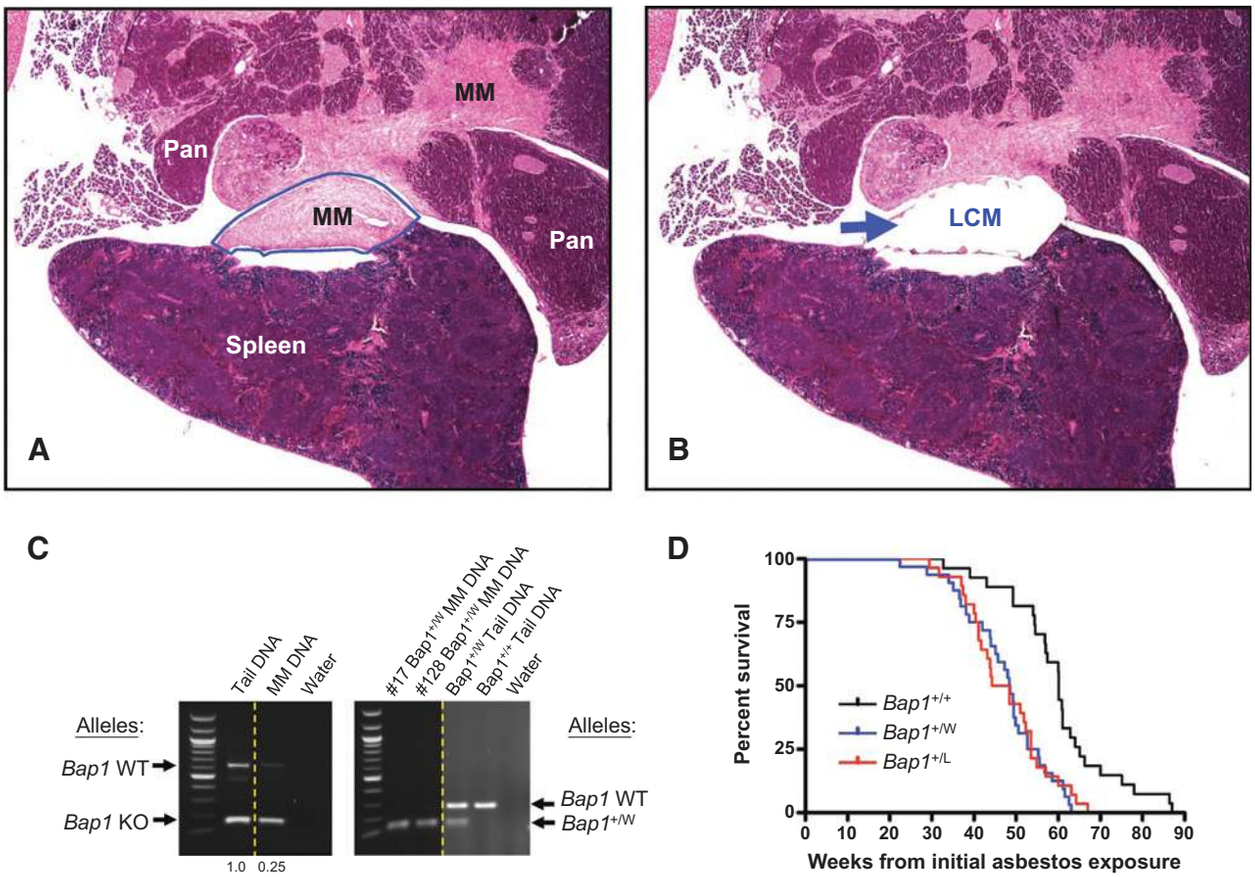

Figure 6.
Spontaneous and asbestos-induced malignant mesothelioma (MM) formation in *Bap1*-mutant mice. A–C, *Bap1* analysis of spontaneous MM from $Bap1^{+/-}$ knockout mouse, in which tumor cells were isolated by LCM. H&E staining of tumor prior to (A) and after (B) LCM. Arrow in B indicates dissected tumor area. Pan, pancreas. Note that the LCM was performed on the same spontaneous MM shown in Fig. 4A–C and Supplementary Fig. S1; the area chosen for LCM was from a serial section of the same tumor area depicted in Supplementary Fig. S1, which confirmed the diagnosis of MMs based on IHC staining and that also revealed loss of nuclear Bap1 staining in many of the tumor cells. Original images presented in A and B, ×20 magnification. C, assessment of *Bap1* allelic loss in LCM-isolated tumor cells from the same spontaneous MM seen in $Bap1^{+/-}$ knockout mouse (left) and from two asbestos-induced MMs from $Bap1^{+/W}$ mice (right). Matching tumor and tail DNA were used as templates to amplify a portion of the mouse *Bap1* gene in the region encompassing exons 6 and 7 (16). Ethidium bromide gel electrophoresis demonstrates markedly reduced residual wild-type (WT) *Bap1* sequences in the spontaneous and asbestos-induced MMs when compared with that of matched tail DNA, indicating that tumor cells have lost the WT *Bap1* allele. The Bio-Rad Quantity One program was used to quantitate the intensities of the PCR products. Left, bands corresponding to larger WT *Bap1* allele (634 bp) and smaller knockout *Bap1* (158 bp) allele, and the ratios of WT to mutant band intensities for each sample are shown below the image. Right, bands representing larger WT *Bap1* allele (~300 bp) and smaller knock-in *Bap1* "W" allele (~150 bp), the latter being a doublet. Mouse numbers 17 and 128 correspond to asbestos-induced MMs from two different $Bap1^{+/W}$ knock-in mice. Dotted lines demarcate lanes from different regions of same gel. D, Kaplan–Meier survival curves showing markedly decreased survival of asbestos-exposed *Bap1*-mutant knock-in cohorts than in asbestos-exposed WT littermates. Survival differences were highly significant ($P < 0.005$ for WT vs. $Bap1^{+/W}$ mice; $P < 0.008$ for WT vs. $Bap1^{+/L}$ mice). Percentage of deaths due to peritoneal MM was 74% in $Bap1^{+/W}$ mice and 71% in $Bap1^{+/L}$ mice compared with 35% of WT animals, which was highly significant ($P < 0.005$ for WT vs. $Bap1^{+/W}$ mice; $P < 0.01$ for WT vs. $Bap1^{+/L}$ mice).

mutant mice exposed to asbestos, indicative of a strong gene–environment interaction. The overall findings are consistent with the notion that *BAP1* mutation carriers are inherently at elevated risk of malignant mesothelioma, and that risk in these individuals increases greatly upon exposure to carcinogenic fibers.

Disclosure of Potential Conflicts of Interest

M. Cheung has ownership interest in a pending patent application (patent publication number US 20140010802). J. Pei has ownership interest in a pending patent for BAP1 mutation testing. J.R. Testa has ownership interest in a pending patent, is a consultant/advisory board member, and has on one occasion provided expert witness testimony. No potential conflicts of interest were disclosed by the other authors.

Authors' Contributions

Conception and design: Y. Kadariya, F.J. Rauscher, J.R. Testa
Development of methodology: Y. Kadariya, M. Cheung, J. Xu, K.Q. Cai, F.J. Rauscher
Acquisition of data (provided animals, acquired and managed patients, provided facilities, etc.): Y. Kadariya, M. Cheung, J. Xu, J. Pei, E. Sementino, C.W. Menges, K.Q. Cai, A.J.P. Klein-Szanto
Analysis and interpretation of data (e.g., statistical analysis, biostatistics, computational analysis): Y. Kadariya, M. Cheung, J. Xu, J. Pei, C.W. Menges, K.Q. Cai, J.R. Testa

Writing, review, and/or revision of the manuscript: Y. Kadariya, M. Cheung, C. W. Menges, K.Q. Cai, F.J. Rauscher, A.J.P. Klein-Szanto, J.R. Testa
Administrative, technical, or material support (i.e., reporting or organizing data, constructing databases): F.J. Rauscher
Study supervision: F.J. Rauscher, J.R. Testa

Acknowledgments

The authors thank Dr. Alfonso Bellacosa for manuscript review and comments. The following FCCC core services assisted this project: Laboratory Animal, Transgenic Mouse, Genomics, Cell Culture, DNA Sequencing, Histopathology, Biosample Repository and Biostatistics and Bioinformatics Facilities.

Grant Support

This work was supported by NIH grants CA-175691 (J.R. Testa and F.J. Rauscher), P42 ES023720 (University of Pennsylvania Superfund Research and Training Program Center project grant to J.R. Testa), CA-06927 (J. Pei, K.Q. Cai, A.J. Klein-Szanto, and J.R. Testa), an Anderson family grant from the Mesothelioma Applied Research Foundation (M. Cheung and J.R. Testa), an appropriation from the Commonwealth of Pennsylvania, and a gift from the Local #14 Mesothelioma Fund of the International Association of Heat and Frost Insulators and Allied Workers.

The costs of publication of this article were defrayed in part by the payment of page charges. This article must therefore be hereby marked *advertisement* in accordance with 18 U.S.C. Section 1734 solely to indicate this fact.

Received December 15, 2015; revised January 12, 2016; accepted January 24, 2016; published online May 2, 2016.

References

1. Testa JR, Malkin D, Schiffman JD. Connecting molecular pathways to hereditary cancer risk syndromes. Am Soc Clin Oncol Educ Book 2013: 81–90.
2. Carbone M, Yang H, Pass HI, Krausz T, Testa JR, Gaudino G. BAP1 and cancer. Nat Rev Cancer 2013;13:153–9.
3. Harbour JW, Onken MD, Roberson ED, Duan S, Cao L, Worley LA, et al. Frequent mutation of BAP1 in metastasizing uveal melanomas. Science 2010;330:1410–3.
4. Testa JR, Cheung M, Pei J, Below JE, Tan Y, Sementino E, et al. Germline BAP1 mutations predispose to malignant mesothelioma. Nat Genet 2011; 43:1022–5.
5. Wiesner T, Obenauf AC, Murali R, Fried I, Griewank KG, Ulz P, et al. Germline mutations in BAP1 predispose to melanocytic tumors. Nat Genet 2011;43:1018–21.
6. Abdel-Rahman MH, Pilarski R, Cebulla CM, Massengill JB, Christopher BN, Boru G, et al. Germline BAP1 mutation predisposes to uveal melanoma, lung adenocarcinoma, meningioma, and other cancers. J Med Genet 2011; 48:856–9.
7. Njauw CN, Kim I, Piris A, Gabree M, Taylor M, Lane AM, et al. Germline BAP1 inactivation is preferentially associated with metastatic ocular melanoma and cutaneous-ocular melanoma families. PLoS One 2012;7: e35295.
8. Wiesner T, Fried I, Ulz P, Stacher E, Popper H, Murali R, et al. Toward an improved definition of the tumor spectrum associated with BAP1 germline mutations. J Clin Oncol 2012;30:e337–40.
9. Popova T, Hebert L, Jacquemin V, Gad S, Caux-Moncoutier V, Dubois-d'Enghien C, et al. Germline BAP1 mutations predispose to renal cell carcinomas. Am J Hum Genet 2013;92:974–80.
10. Aoude LG, Wadt K, Bojesen A, Cruger D, Borg A, Trent JM, et al. A BAP1 mutation in a Danish family predisposes to uveal melanoma and other cancers. PLoS One 2013;8:e72144.
11. Cheung M, Talarchek J, Schindeler K, Saraiva E, Penney LS, Ludman M, et al. Further evidence for germline BAP1 mutations predisposing to melanoma and malignant mesothelioma. Cancer Genet 2013;206:206–10.
12. Wadt KA, Aoude LG, Johansson P, Solinas A, Pritchard A, Crainic O, et al. A recurrent germline BAP1 mutation and extension of the BAP1 tumor predisposition spectrum to include basal cell carcinoma. Clin Genet 2015; 88:267–72.
13. Cheung M, Kadariya Y, Talarchek J, Pei J, Ohar JA, Kayaleh OR, et al. Germline BAP1 mutation in a family with high incidence of multiple primary cancers and a potential gene-environment interaction. Cancer Lett 2015;369:261–5.
14. Knudson AGJr. Mutation and cancer: statistical study of retinoblastoma. Proc Natl Acad Sci U S A 1971;68:820–3.
15. Dey A, Seshasayee D, Noubade R, French DM, Liu J, Chaurushiya MS, et al. Loss of the tumor suppressor BAP1 causes myeloid transformation. Science 2012;337:1541–6.
16. Xu J, Kadariya Y, Cheung M, Pei J, Talarchek J, Sementino E, et al. Germline mutation of Bap1 accelerates development of asbestos-induced malignant mesothelioma. Cancer Res 2014;74:4388–97.
17. Napolitano A, Pellegrini L, Dey A, Larson D, Tanji M, Flores EG, et al. Minimal asbestos exposure in germline BAP1 heterozygous mice is associated with deregulated inflammatory response and increased risk of mesothelioma. Oncogene. 2015 Jun 29. [Epub ahead of print].
18. Qin J, Zhou Z, Chen W, Wang C, Zhang H, Ge G, et al. BAP1 promotes breast cancer cell proliferation and metastasis by deubiquitinating KLF5. Nat Commun 2015;6:8471.
19. Bott M, Brevet M, Taylor BS, Shimizu S, Ito T, Wang L, et al. The nuclear deubiquitinase BAP1 is commonly inactivated by somatic mutations and 3p21.1 losses in malignant pleural mesothelioma. Nat Genet 2011;43: 668–72.
20. Meyer M, de Angelis MH, Wurst W, Kühn R. Gene targeting by homologous recombination in mouse zygotes mediated by zinc-finger nucleases. Proc Natl Acad Sci U S A 2010;107:15022–6.
21. Altomare DA, Vaslet CA, Skele KL, De Rienzo A, Devarajan K, Jhanwar SC, et al. A mouse model recapitulating molecular features of human mesothelioma. Cancer Res 2005;65:8090–5.
22. Altomare DA, Menges CW, Pei J, Zhang L, Skele-Stump KL, Carbone M, et al. Activated TNF-alpha/NF-kappaB signaling via down-regulation of Fas-associated factor 1 in asbestos-induced mesotheliomas from Arf knockout mice. Proc Natl Acad Sci U S A 2009;106:3430–5.
23. McClatchey AI, Saotome I, Mercer K, Crowley D, Gusella JF, Bronson RT, et al. Mice heterozygous for a mutation at the *Nf2* tumor suppressor locus develop a range of highly metastatic tumors. Genes Dev 1998;12:1121–33.
24. Park MS, Rosai J, Nguyen HT, Capodieci P, Cordon-Cardo C, Koff A. p27 and Rb are on overlapping pathways suppressing tumorigenesis in mice. Proc Natl Acad Sci U S A 1999;96:6382–7.
25. Thrall MM, Paley P, Pizer E, Garcia R, Goff BA. Patterns of spread and recurrence of sex cord-stromal tumors of the ovary. Gynecol Oncol 2011;122:242–5.